TRUSS-ANALOGY METHOD FOR THE ANALYSIS

OF STEEL DIAPHRAGM

By

SHEN-SHENG A. CHOU

Diploma

Taiwan Provincial Taipei Institute

of Technology

Taipei, Taiwan, Republic of China

1969

Submitted to the Faculty of the Graduate College
of the Oklahoma State University
in partial fulfillment of the requirements
for the Degree of
MASTER OF SCIENCE
December, 1974

TRUSS-ANALOGY METHOD FOR THE ANALYSIS

OF STEEL DIAPHRAGM

Report Approved:

Duane S. Ellifritt

Report Adviser

John P. Lloyd

A E Kelly

D N Durham

Dean of the Graduate College

ACKNOWLEDGMENTS

In the final preparation of this report, I would like to express my sincere gratitude to the following:

To my major adviser, Dr. Duane S. Ellifritt, for his assistance and guidance throughout the preparation of this report;

To all the professors in the School of Civil Engineering for their valuable instruction and friendliness throughout my years of study at this institution;

Finally, to my parents, sister, for their support and encouragement during my studies.

TABLE OF CONTENTS

Chapter Page

I. INTRODUCTION 1

1.1 General 1
1.2 Brief Description of West Virginia Tests 2
1.3 Scope and Objective of Investigation 2

II. APPROACH OF TRUSS-ANALOGY METHOD 7

III. DESCRIPTION OF THE TRUSS-ANALOGY METHOD 9

IV. CORRELATION WITH TEST RESULTS 12

V. MATHEMATICAL MODELS 21

5.1 General 21
5.2 Limitations of the Mathematical Models 21

VI. SUMMARY AND CONCLUSIONS 27

VII. RECOMMENDATIONS FOR FUTURE RESEARCH 29

REFERENCES 31

APPENDIX - "STRUDL" COMPUTER INPUT LIST 32

LIST OF FIGURES

Figure		Page
1.	Diaphragm Test Frame	3
2.	Welding Steel Deck to Test Frame	4
3.	Diaphragm Loading Device	5
4.	Bryan Test Specimen	8
5.	Relationship Between Diagonal Stresses and Shear Load . . .	8
6.	Illustration Example	11
7.	Through 15. Correlation Curves	13 - 20
16.	Cross-Section Area V.S. L/T Ratio	22
17.	Buckling Load V.S. L/T Ratio	23
18.	Effectiveness of Steel Deck Illustration	30
19.	Typical Configuration of Truss Analogy	32

CHAPTER I

INTRODUCTION

1.1 General

The behavior of light gage steel panel diaphragms does not yield nicely to analysis. The large number of relatively small parts involved, with possible individual movement, and the stress concentrations that are present near the welds as local buckling and tearing around welds when horizontal load is applied, prevent the application of conventional methods of analysis with large degree of confidence. Accordingly, a considerable number of isolated tests have been performed by a number of persons and institutions over a period of time.

Among these tests, the most recent were conducted by the Department of Civil Engineering of West Virginia University in the late 1960's. There followed an extended series of more than one hundred diaphragm tests, utilizing many types of panels, steel thickness, patterns of welds, panel spans, and panel depths. Information that has evolved from these tests has provided a firm basis for the design and installation of light gage steel diaphragms in many parts of the country. Ultimate strength and working strength values have been established for many different systems, and the performance of such diaphragms under load has been accurately cataloged.

All the mathematical models developed in this report are adjusted according to these test results.

1.2 Brief Description of West Virginia Tests

At West Virginia University a large-scale diaphragms testing program was begun in 1967. Tests were made on 16, 18, 20, and 22 gage decks with lengths of 12, 16 and 20 feet long. Panel widths tested were 18, 24, 30, and 36 inches. All tests were made on a horizontal cantilever test frame, illustrated in Figure 1. Connections between the perimeter members of the frame, as well as connections at the purlin ends, were made with light clip angles and bolts. The entire frame assembly was supported on a roller system and could be moved easily prior to attaching the deck, indicating that all interior connections could be considered pinned. The steel deck was then welded to the frame, thus creating a shear-rigid diaphragm (see Figure 2). The diaphragm was then loaded in its plane by a hydraulic jack and load cell arrangement in line with the free edge (Figure 3). Load was applied in increments from zero to failure with deflection measurements made at each stage of loading. For more detail arrangement and test procedures, see Reference 1.

1.3 Scope and Objective of Investigation

Tested diaphragms were evaluated with respect to two major behavioral parameters, ultimate strength and shear stiffness. From the West Virginia University research, it is apparent that strength and stiffness are primarily influenced by sheet thickness, purlin spacing, panel width, panel length, yield strength of material, deck shape, fastener type, and arrangement. The purpose of this report is to develop a truss-analogy method to determine these two parameters in

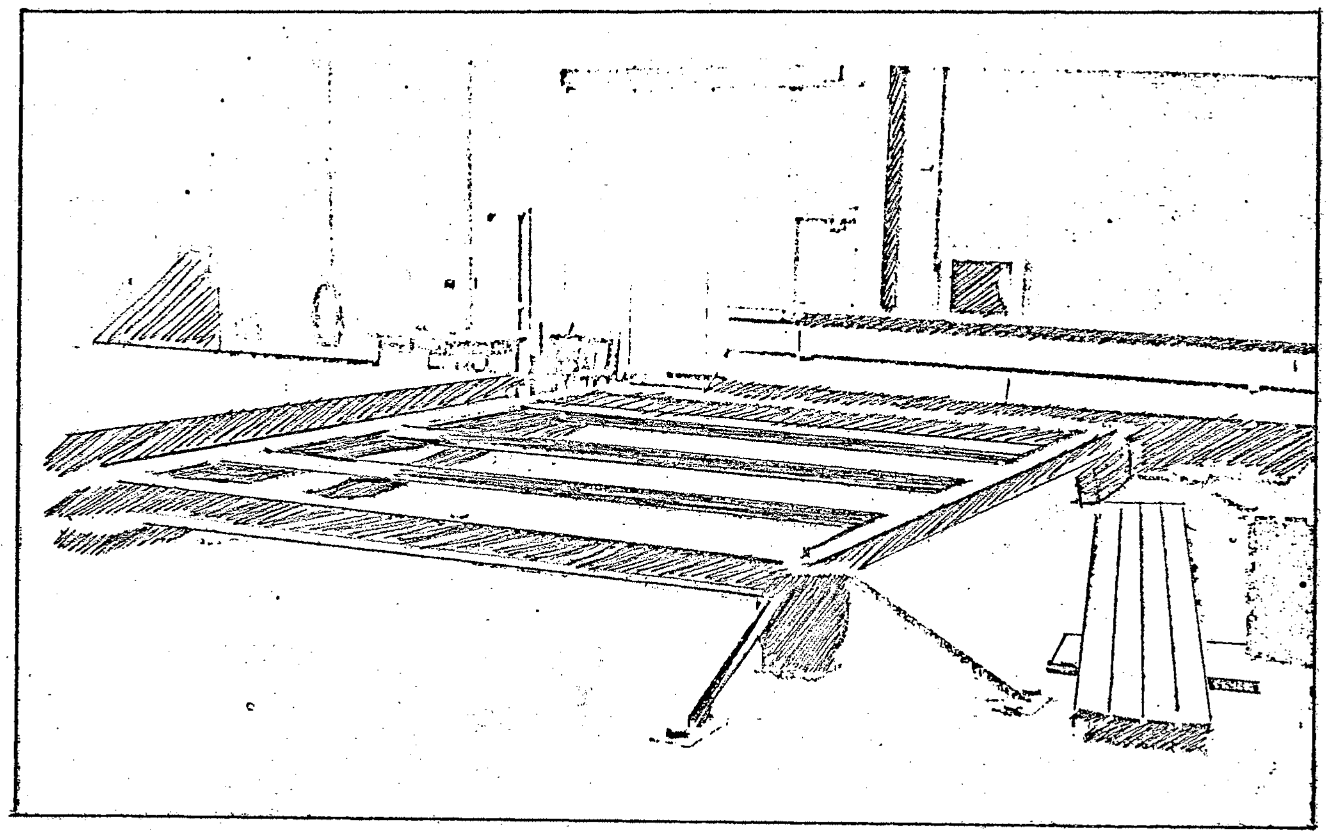

Figure 1. Diaphragm Test Frame

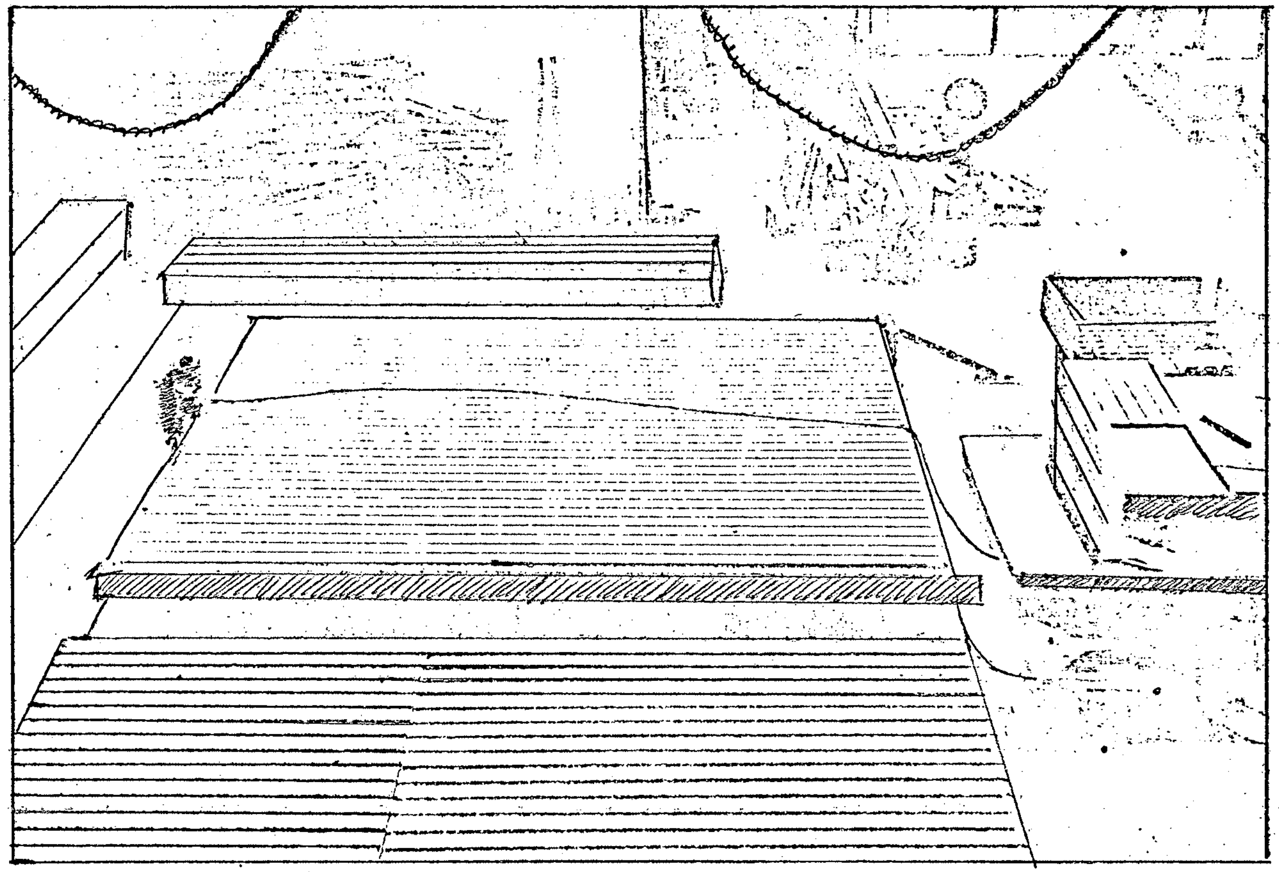

Figure 2. Welding Steel Deck to Test Frame

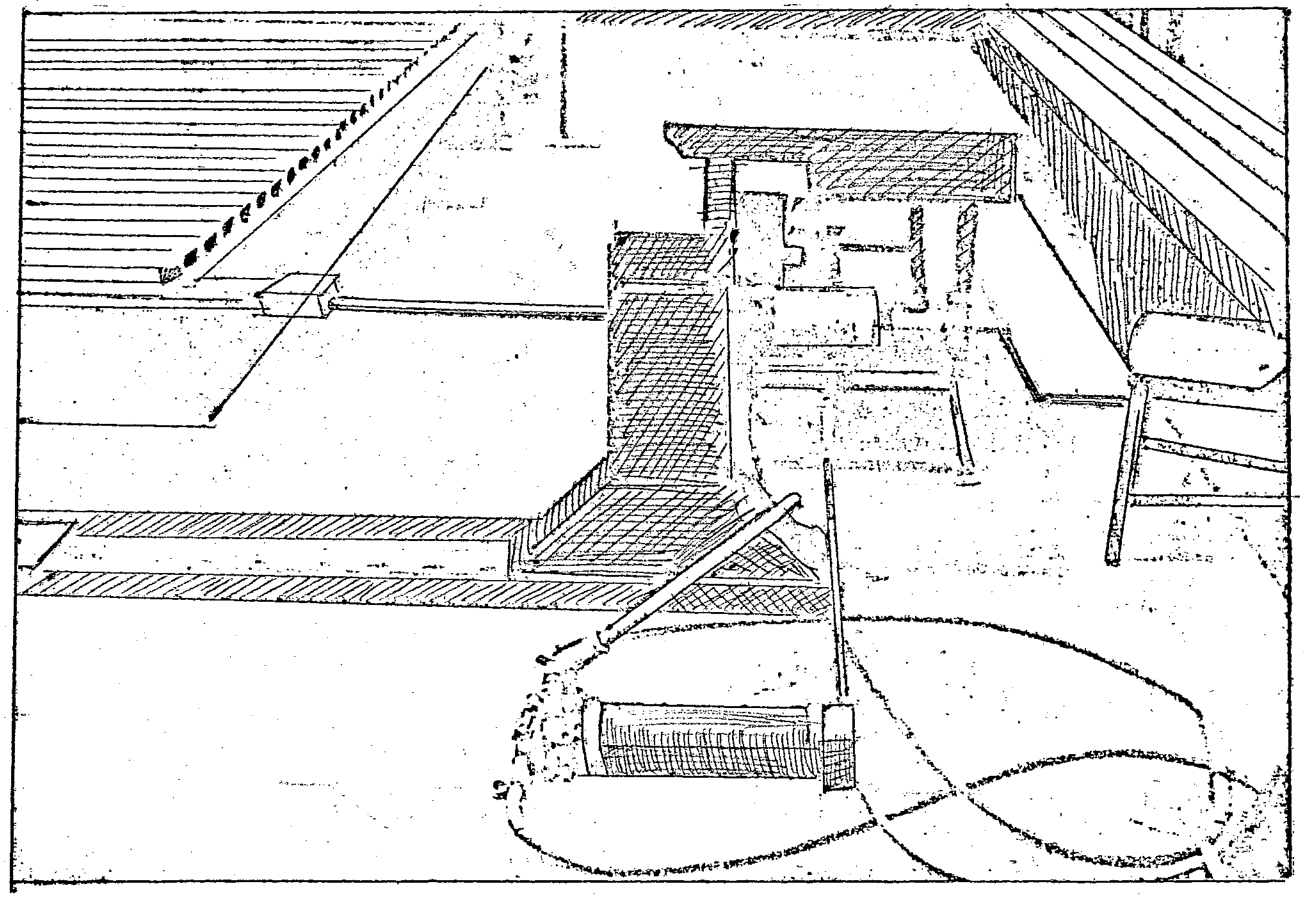

Figure 3. Diaphragm Loading Device

terms of the most significant of the variables mentioned above. The report is divided into sections covering the approach of the truss-analogy method, description of the method, development of empirical equations, correlations with test data, and conclusions. An example problem is included in the Appendix.

CHAPTER II

APPROACH OF TRUSS-ANALOGY METHOD

In 1964, Eric R. Bryan conducted a series of tests on shear of thin plates. The apparatus consisted of an aluminum sheet, 18 inches by 12 inches by 0.01 inches thick. The edge members, also of aluminum, are pinned at the corners (as shown in Figure 4) so that all the shear is carried by the sheet. There are four strain gages attached in tensile diagonal and compressive diagonal directions. A plot of test results which indicates the relationship between shear load Q and diagonal stresses is shown in Figure 5.

It can be seen that, after buckling, the compressive stresses do increase because of the restraint of tensile field, but at a much lower rate than the tensile stresses. They also become asymptotic to a certain value, whereas the tensile stresses continue to increase. As a result, the compressive stress, after buckling, is a small percentage of the tensile stress as the external load is increased. Consequently, the excessive compressive stress then is carried by its panel edge members. If the panel edge member is a part of the steel deck itself, which will be discussed later, the buckling failure will be the panel edge flute buckling failure.

Based on the above analysis, the truss-analogy approach, with compressive diagonal members ignored, is constructed.

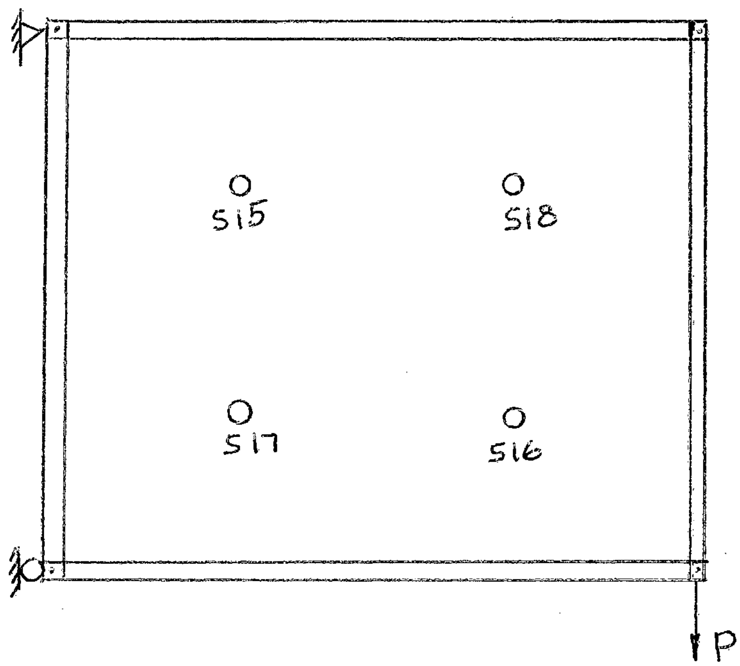

Figure 4. Bryan Test Specimen

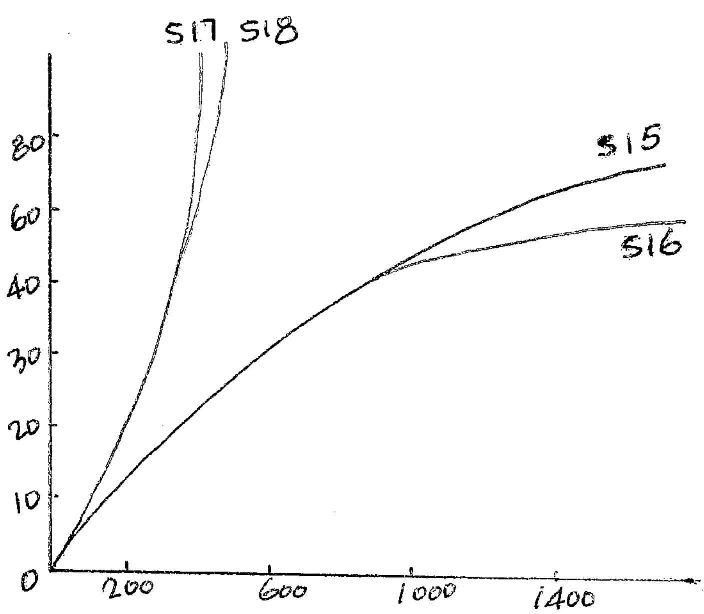

Figure 5. Relationship Between Diagonal Stresses and Shear Load

CHAPTER III

DESCRIPTION OF THE TRUSS-ANALOGY METHOD

Since the truss-analogy structure is a highly statically indeterminate structure, it is desirable to use a computer to solve. As far as I know, there are two computer programs available; these are "Plane Frame and Truss Program" and "STRUDL" program. The former limits the number of truss members to not more than 400 and joints to not more than 200. In this report "STRUDL" is used. The following steps are used in the analytical procedures.

1. Set up a "STRUDL" coordinates system as shown in Figures 6 and 7.

2. All the member property input data are known except the cross-section of those imaginary internal truss members. A value for that was first assumed and this value could easily be adjusted later, because in the elastic medium the deflection of a member is directly proportional to its sectional area. Equation (1) shows the relationship between cross-sectional area, a, and deflection:

$$\frac{\Delta_t}{A_t} = \frac{\Delta_c}{A_c} \qquad (1)$$

where Δ_t is the test data deflection, A_c is the assumed computer input data, A_t is the cross-sectional area needed, and Δ_c is the computer output result of deflection corresponding to A_c. Figure 17 is the plot of cross section, V.S. L/T ratio.

3. After the cross-sectional area of the diagonal has been determined, assume values of the buckling force and ultimate tensile force in the diagonal, then compare computer deflection results with test results. If the test results do not agree, readjust the previous assumptions. Continue this trial-and-error process until the computer results fit the test results in an acceptable region. Figure 18 is the plot of buckling force in compressive member V.S. L/T ratio.

4. As the trial-and-error process continued, it was found that after the steel deck was torn off around the welds, namely when the ultimate tensile force had been reached, it still resisted some force. This phenomenon can be explained: when one steel deck panel was torn off, the adjacent welds picked up the load that had formerly been carried by the weld that failed. Therefore, when any member reached its ultimate tensile force, it was taken out and fifty percent of its ultimate tensile force was applied to that joint in the direction of that member in the next computer run. On the other hand, when a member buckled, it was merely taken out (see Figure 8).

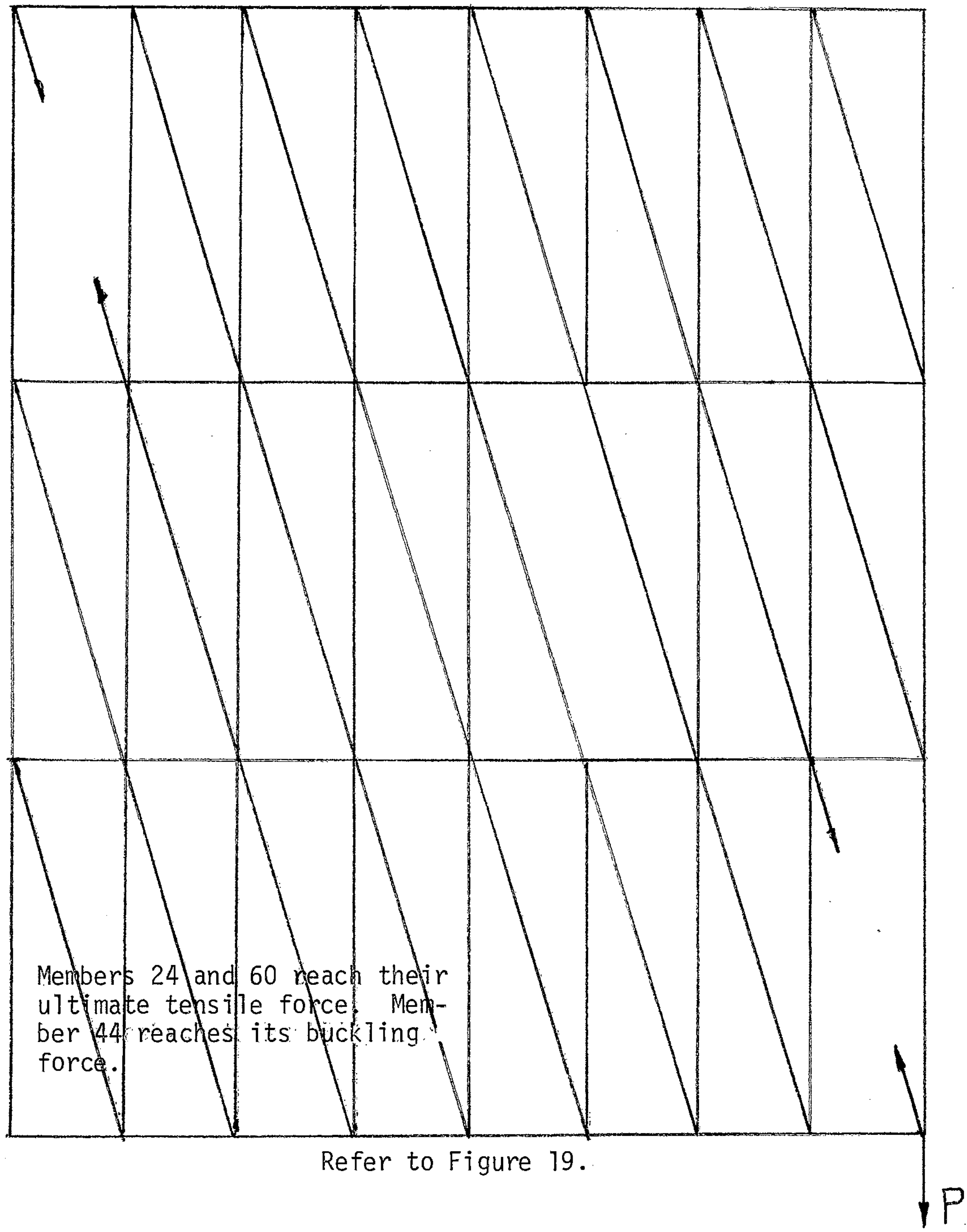

Figure 6. Illustration Example

CHAPTER IV

CORRELATION WITH TEST RESULTS

The following are ten correlation plots. From these plots, it is seen that the computer input assumptions are well confirmed.

The designations on the test curves, such as W-3, refer to tests made at West Virginia University.

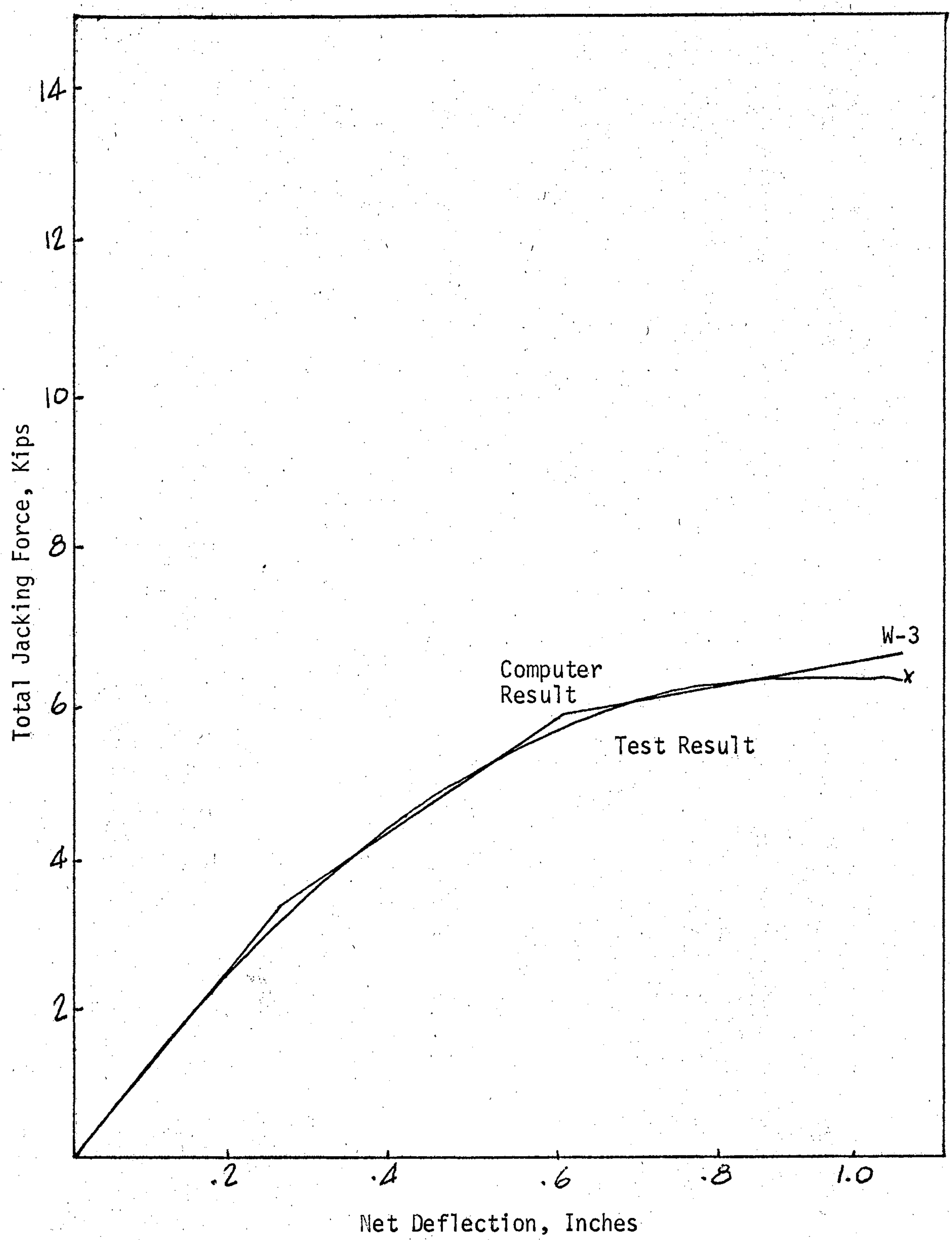

Figure 8. Correlation Curves

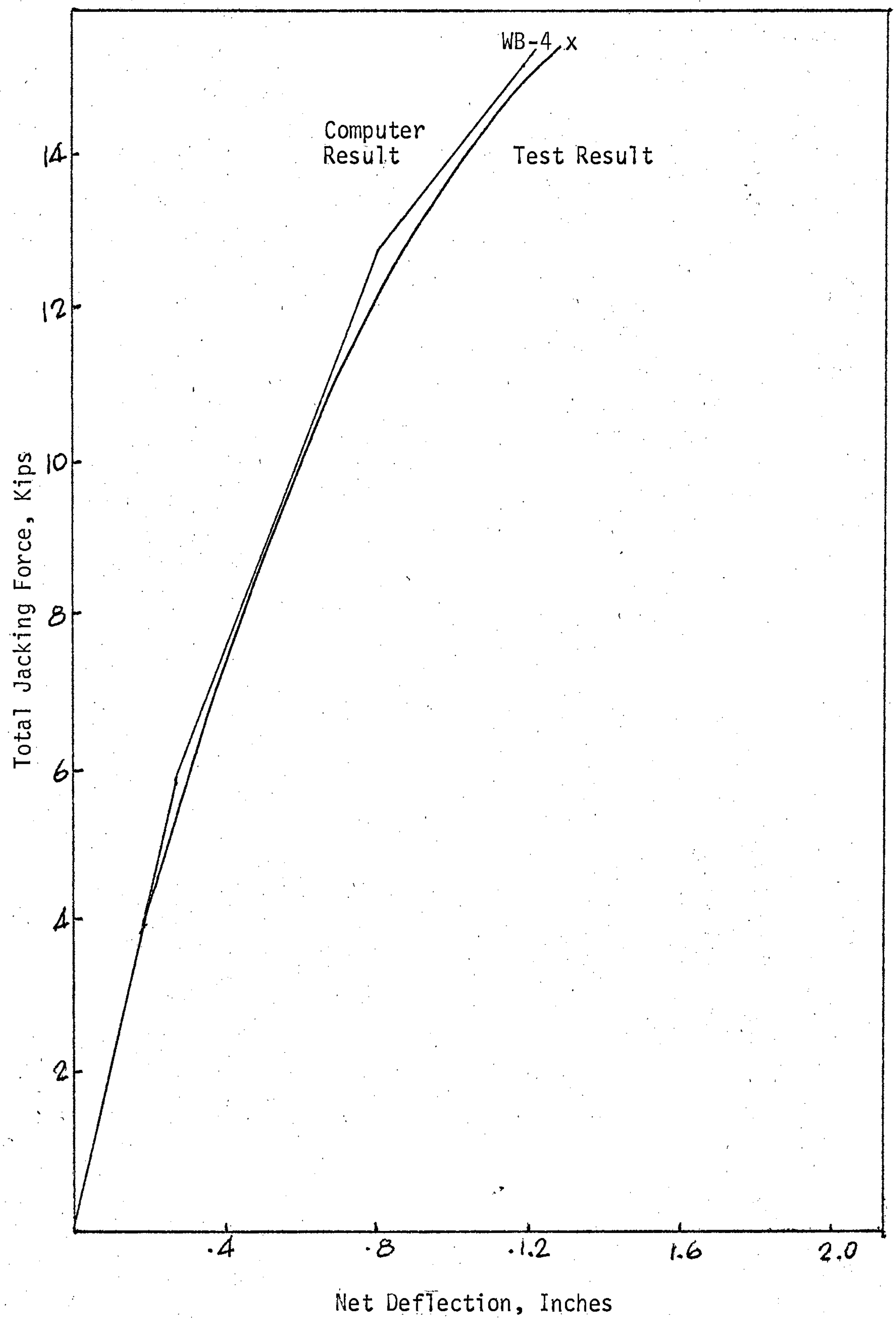

Figure 9. Correlation Curves

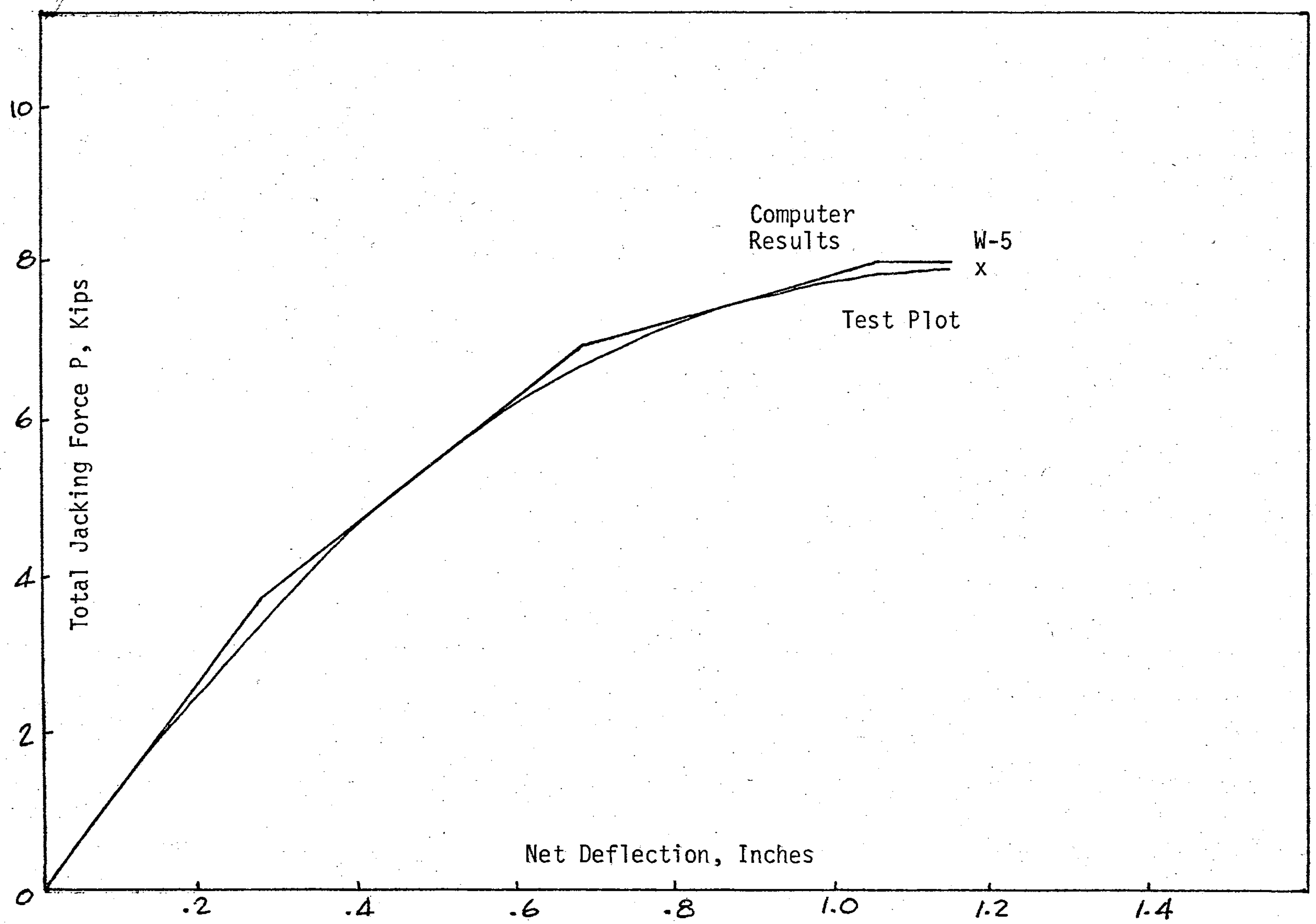

Figure 10. Correlation Curves

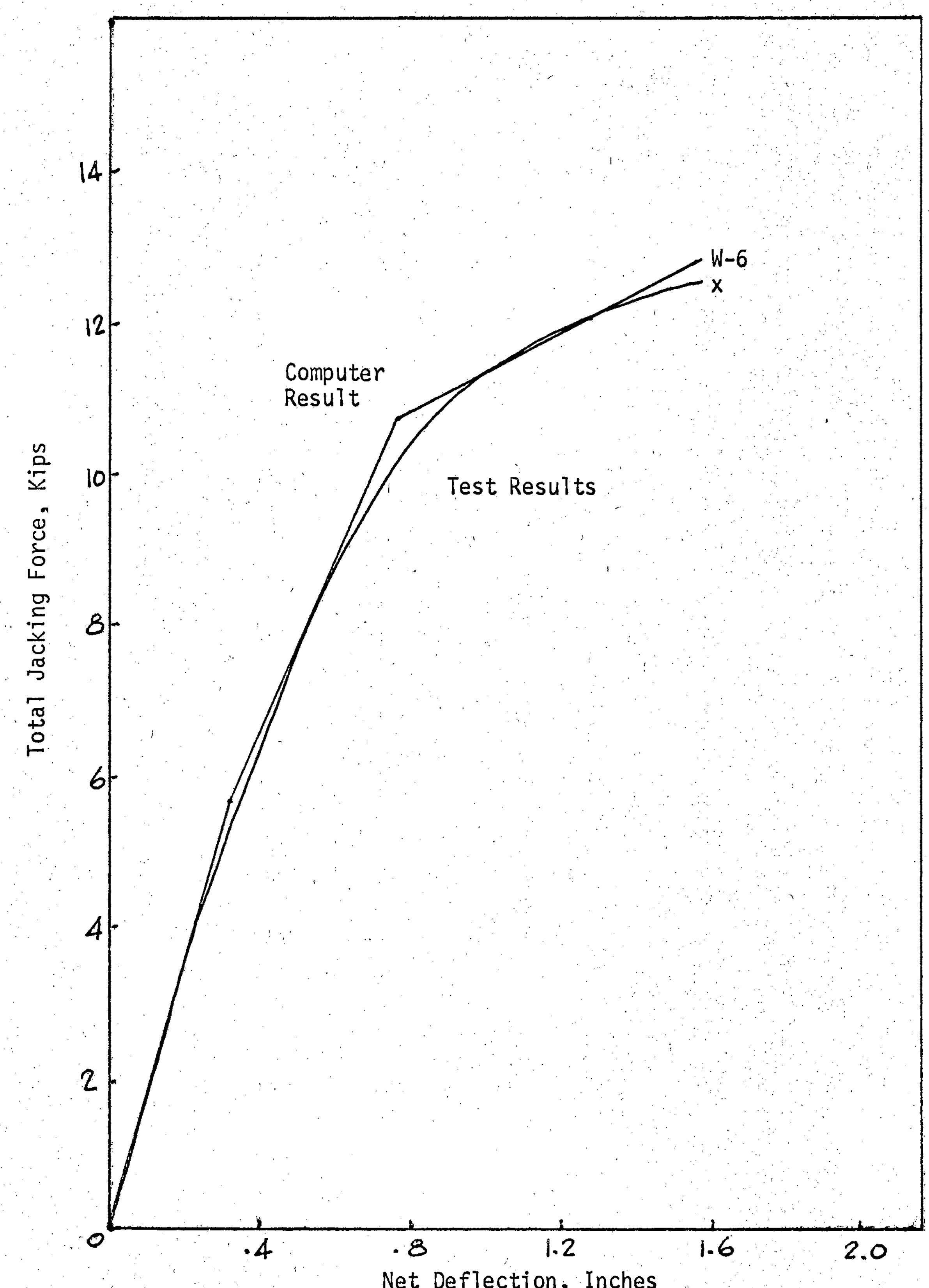

Figure 11. Correlation Curves

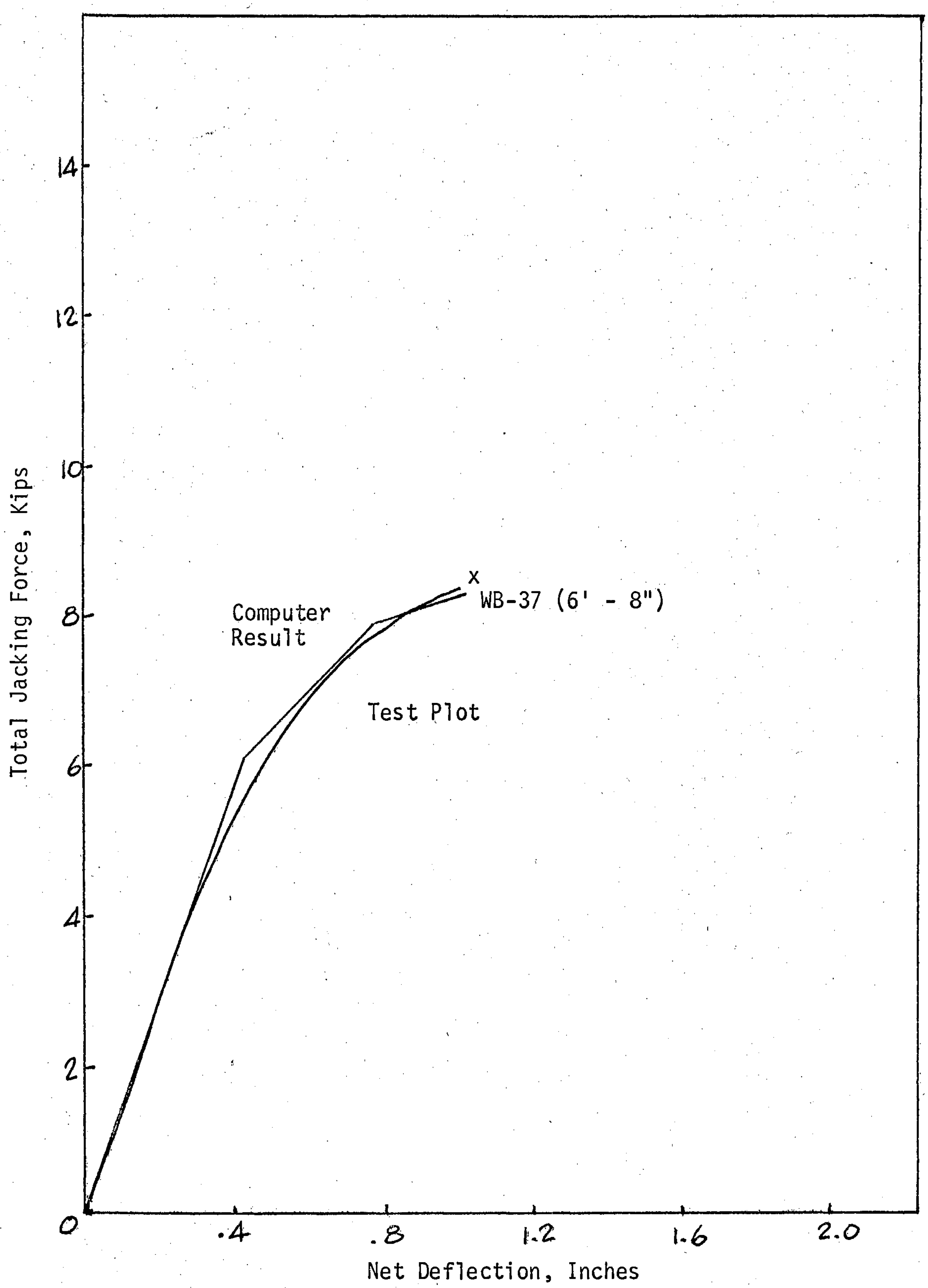

Figure 12. Correlation Curves

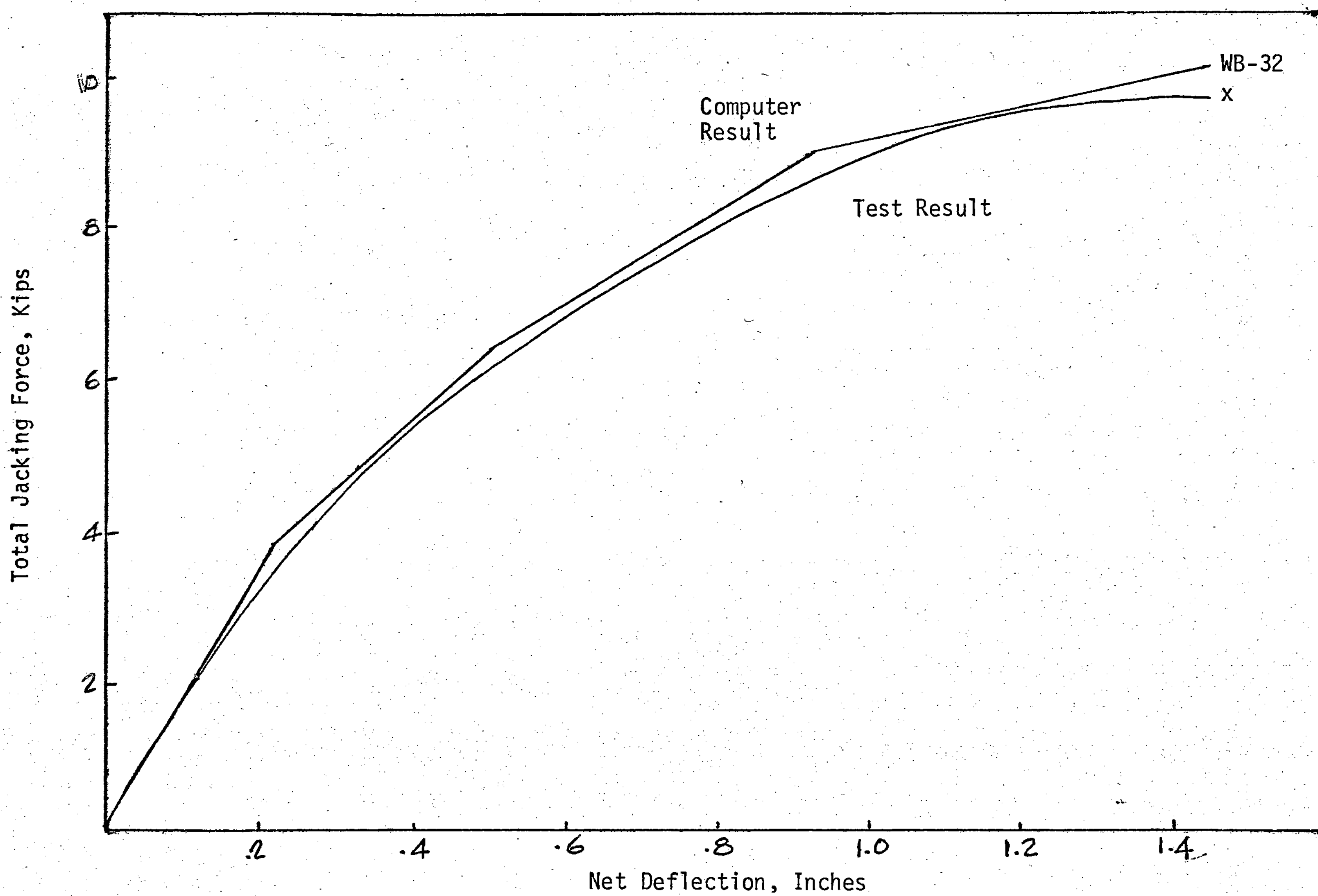

Figure 13. Correlation Curves

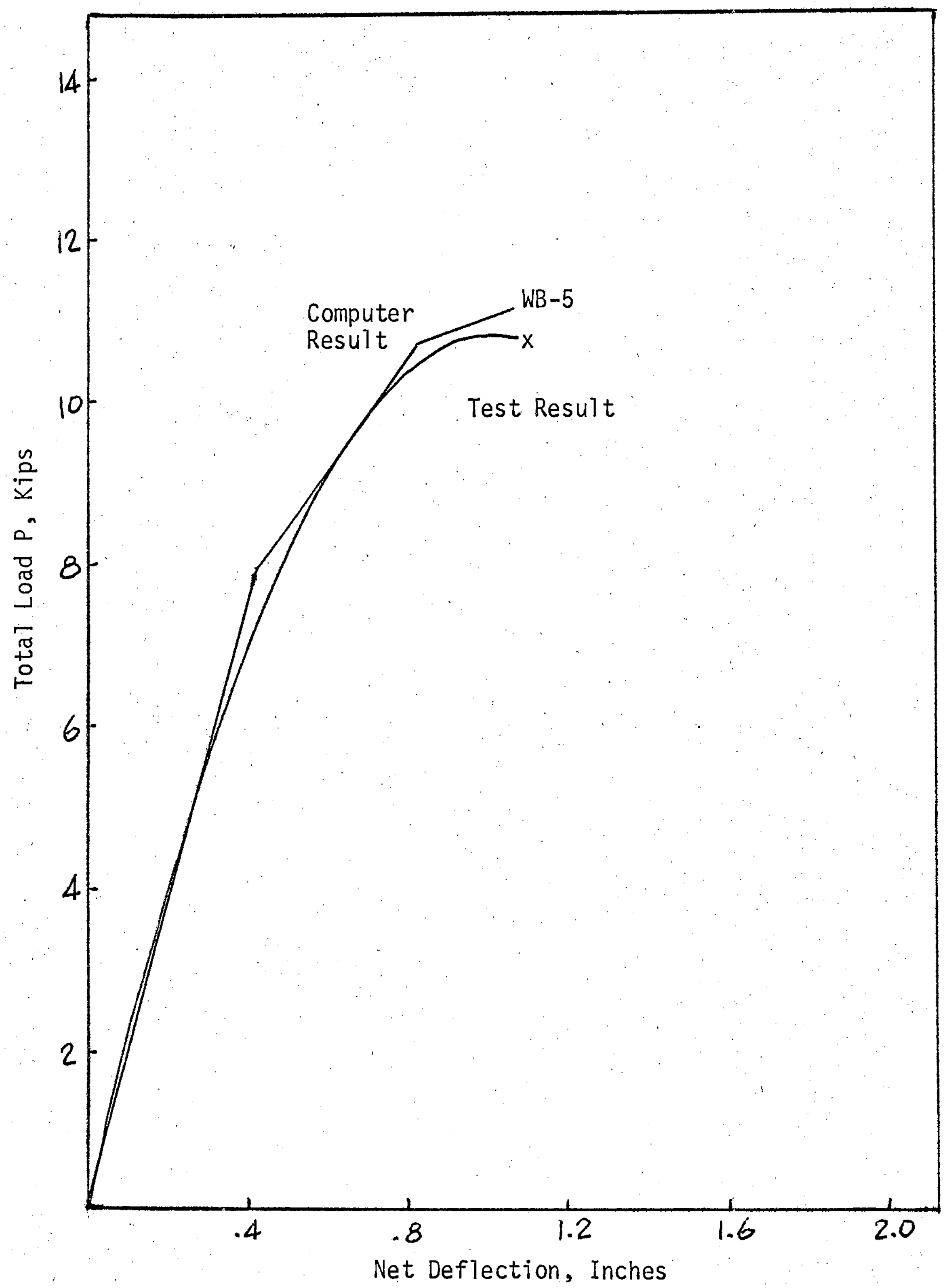

Figure 14. Correlation Curves

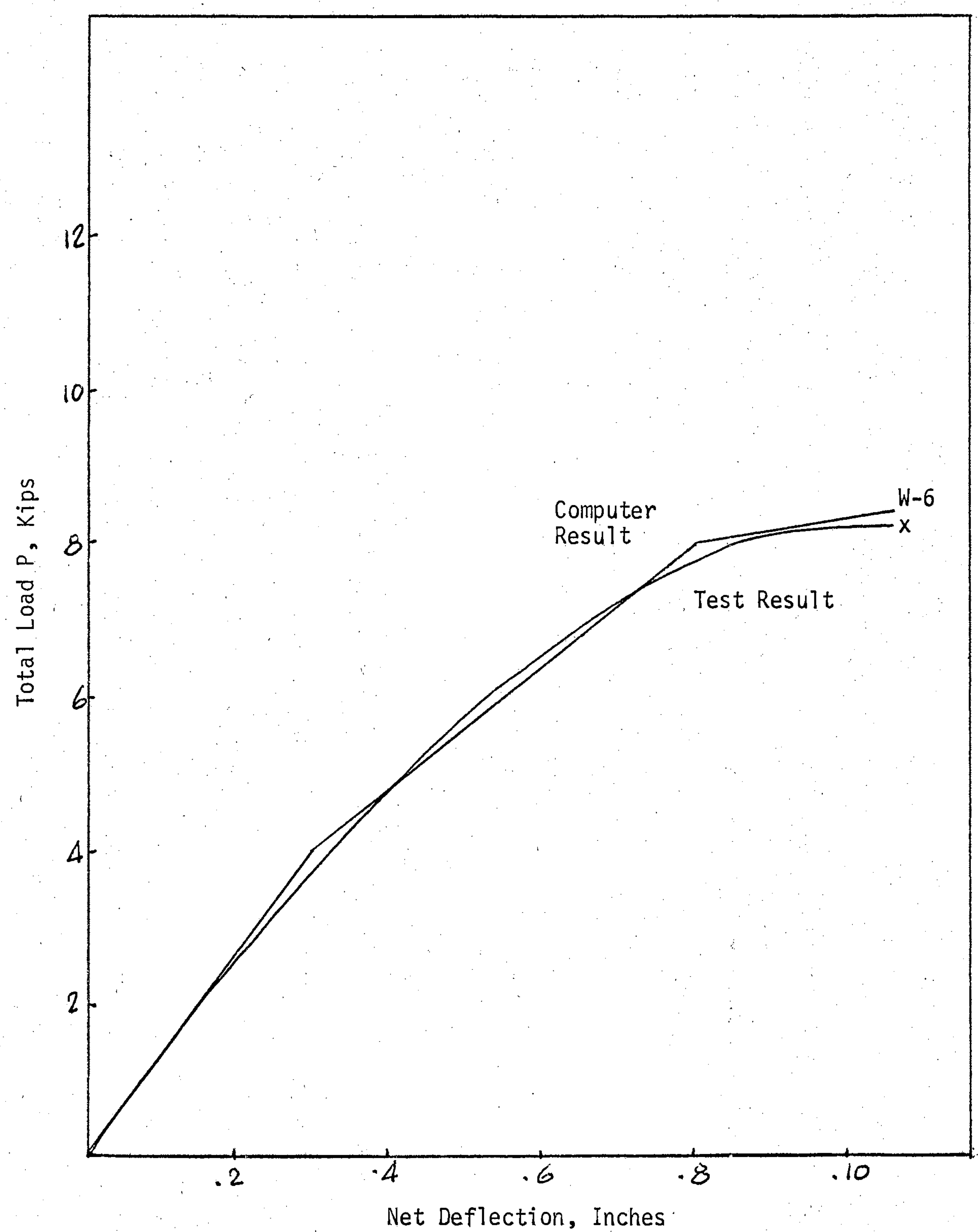

Figure 15. Correlation Curves

CHAPTER V

MATHEMATICAL MODELS

5.1 General

Since the length of purlin spacing, L, and the thickness of steel decks are the dominating parameters of shear strength of steel diaphragms, so the values of the section area, buckling force and ultimate tensile force equations herein are all expressed in terms of L/t ratio. All data curves are so plotted by using second order parabolic interpolation.

5.2 Limitations of the Mathematical Models

The mathematical models are:

1. Valid for W and WB type decks.
2. Used for standard weld patterns only.

Since the L/t ratio of the test steel diaphragms were ranged from 1000 to 3000, the mathematical models obtained from Figure 18 will be considerably accurate when L/t ratio within that range. The following equations are to the steel deck type specified as 22, 20 and 18 gage deck.

For 22 gage deck: (From L/t = 1300 to L/t = 3000)

$$a = 1.732 \times 10^{-7} L^2 t^{-2} + 89.7 \times 10^{-5} L t^{-1} - 0.974.$$

For 20 gage deck: (From L/t = 1000 to L/t = 3000)

$$a = -1.665 \times 10^{-7} L^2 t^{-2} + 68.57 \times 10^{-5} L t^{-1} - 0.478.$$

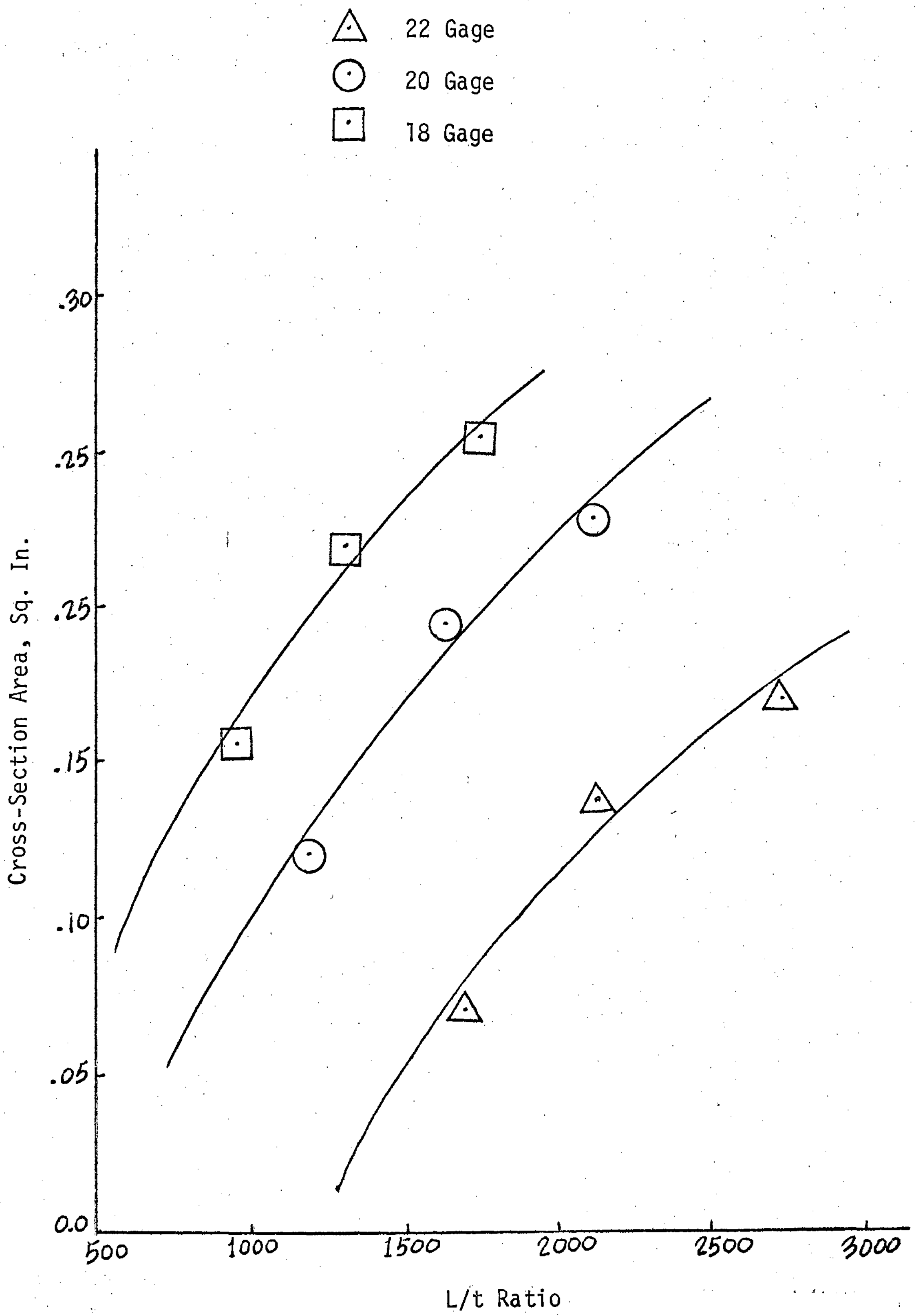

Figure 16. Cross-Section Area Versus L/t Ratio

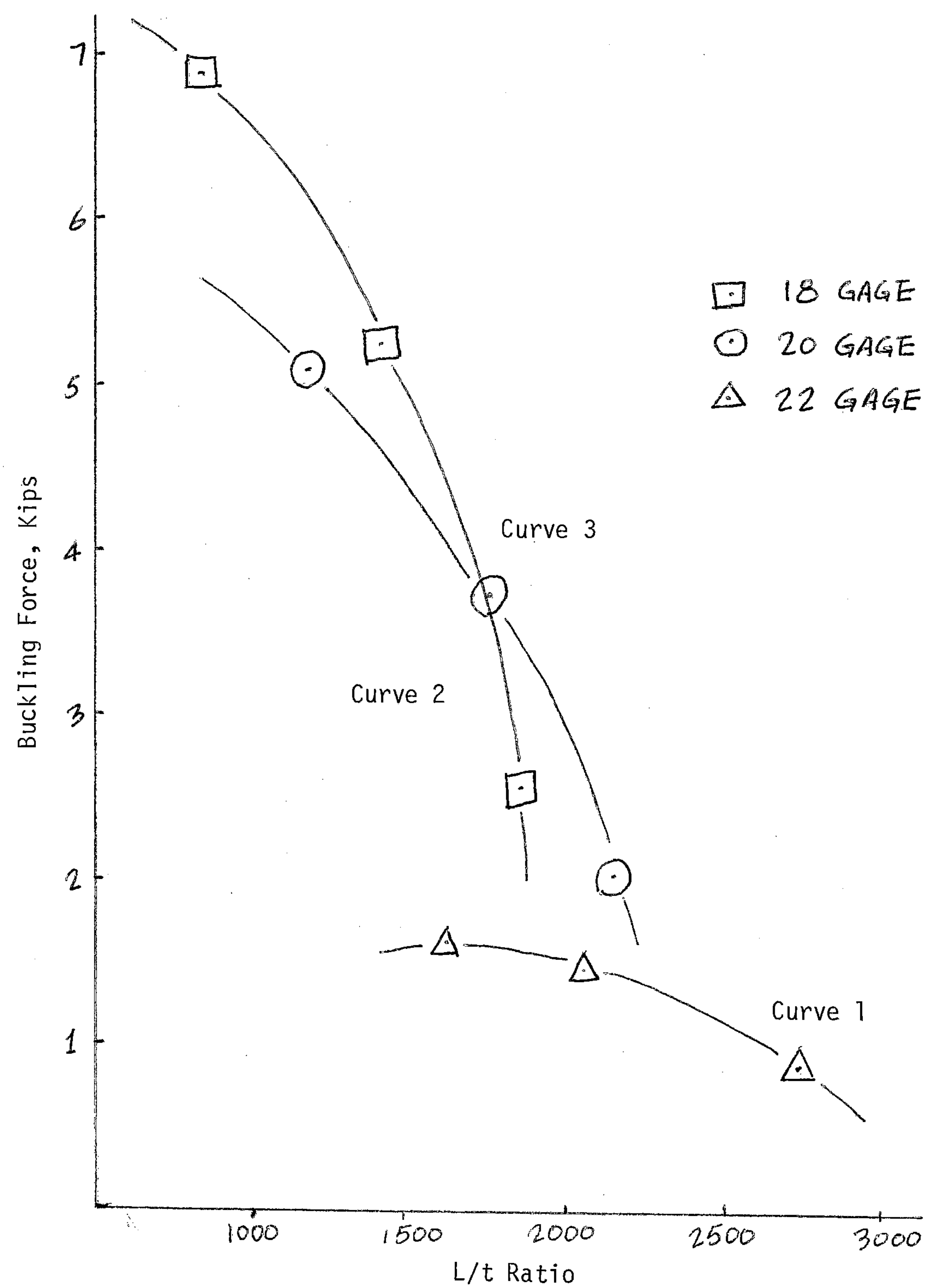

Figure 17. Buckling Loads Versus L/t Ratio

For 18 gage deck: (From $L/t = 500$ to $L/t = 2500$)

$$a = -2.74 \times 10^{-7} L^2 t^{-2} + 87.64 \times 10^{-5} L t^{-1} - 0.442.$$

Apparently, the member buckling force plotted in Figure 17 is the combination of the effects of local buckling and overall buckling. Since the steel deck is formed by a piece of thin steel plate, the thickness of the deck strongly influences the magnitude of local buckling load prior to overall buckling.

As it was pointed out in the introduction of this report, the behavior of light gage panel diaphragms does not yield nicely to analysis because the large number of relatively small parts involved. One of the most important properties among those small parts is the quality of welding which was assumed perfect in this method. Consequently, the buckling forces were obtained on the basis of this assumption.

Even though the quality of welding was inspected in the laboratory, it is necessary to investigate how good that assumption is, as far as the determination of buckling forces is concerned.

AISC presents an interaction diagram of axial force Q versus $(b/t)\sqrt{fy}$ shown below. It indicates that when $b/t \sqrt{fy} \geq 200$, the capacity of resisting axial load decreases to about 20 percent of its capacity when $b/t \sqrt{fy} \leq 100$, and remains a low limit up to $b/t \sqrt{fy} = 300$. In our case, assume $b/t \sqrt{fy} = 330$ for 22 gage deck. Curve 1 represents 22 gage which is rather flat regardless of length L, so this conforms with the AISC curve.

For curve 2, $b/t \sqrt{fy} = 180$, which represents 20 gage deck which is controlled by both $(b/t)\sqrt{fy}$ ratio and Euler's $1/L^2$ ratio. Since $(b/t)\sqrt{fy}$ ratio of 18 gage and 20 gage are both in the range of 100 to

200, from AISC's curve, the slope in this range is almost constant as is that in Figure 17.

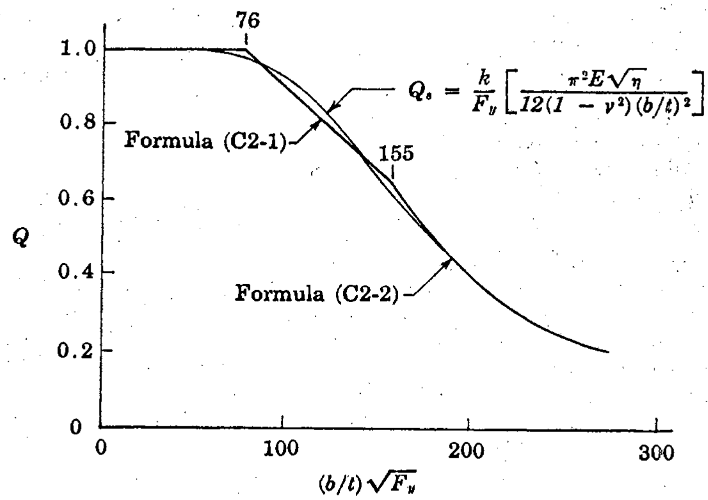

The lowest point of each curve represents when L = 6.8 feet, the second lower point represents L = 5', and the highest point represents L = 4'. From curves 2 and 3, it can be seen that the buckling force almost doubles as L decreases from 4' to 5' or from 5' to 6.8', which is consistent with the AISC column strength curve.

The following are the equations for 22, 20 and 18 gage deck separately:

22 Gage: (L/t ratio from 1500 to 2750)

$$Fa = -0.432\ 10^{-6}\ L^2\ t^{-2} + 13.79\ 10^{-4}\ L\ t^{-1} + 0.501.$$

20 Gage: (L/t ratio from 1000 to 2500)

$$Fa = 1.178\ 10^{-6}\ L^2\ t^{-2} - 77.18\ 10^{-4}\ L\ t^{-1} + 13.29.$$

18 Gage: (L/t ratio from 800 to 2000)

$$Fa = 3.474\ 10^{-6}\ L^2\ t^{-2} - 159\ 10^{-4}\ L\ t^{-1} + 19.51.$$

Ultimate tensile force of truss member:

$$T = 3.50\ t/.036.$$

CHAPTER VI

SUMMARY AND CONCLUSIONS

When the analytical results for the truss-analogy model were compared with the test data, four conclusions were reached:

1. The truss-analogy method provides some important information; that is, the stresses in steel decks are due to external in-plane load. From this additional information a designer can visualize what portions of a diaphragm are critical, and can predict how the stress of one deck panel is transmitted to adjacent panels after that panel fails.

2. This method is a valuable and rather unique way to solve a steel deck floor or roof with openings by removing members in absent panel areas during analysis.

3. It can be a tool for a designer to anticipate the capacity of a steel diaphragm which has already been built and contains some defective welds due to imperfect workmanship.

4. The mathematical expressions for calculating buckling load and ultimate tensile load have been developed in this method. After these two values of a particular design case have been obtained, it is justified and desirable for a designer to decide whether the extra welds are needed to strengthen the diaphragm by comparing the buckling force and ultimate tensile force. In other words, it would be senseless to do so if the buckling force controls.

Throughout the above four conclusions, it can be seen that the advantage of this method is to provide knowledge of how steel diaphragms behave under in-plane force and how to attack some design cases with configurations other than a rectangular shape.

CHAPTER VII

RECOMMENDATIONS FOR FUTURE RESEARCH

The following recommendations are offered for future research:

1. In many structures, shear-resistant light gage metal diaphragms are connected directly to beams or columns of the steel framework, and may continuously brace these members along their length. The light-gage wall cladding on a building frame, for example, can brace the columns against weak axis buckling if adequate connection is provided between the columns and the diaphragm. Similarly, light-gage steel roof or floor decking can restrain lateral buckling of truss chords, beams and purlins. This action of the diaphragm in bracing individual members has been investigated by Cornell University in 1967. However, if the truss-analogy method can be developed for buckling-restraint diaphragms, the advantages are obvious as indicated in the previous conclusions.

2. As in practice, the edge members of a light-gage diaphragm can be connected in several fashions, such as two corners pinned with the other two corners rigid or even semi-rigid. Suppose there was a four-corner, rigid-connected diaphragm, as shown in Figure 18 (the dotted line indicates the deflection curve under load P). As you can see, the steel deck in Zones 1 and 3 experience little shear strain. In other words, only the steel deck in Zone 2 was resistant to shear force. Therefore, what proportion of the shear capacity, after all corners

pinned shear diaphragm have been taken into account, is in question. After this question has been answered, the truss-analogy method can then be applied by removing members in Zone 1 and 3.

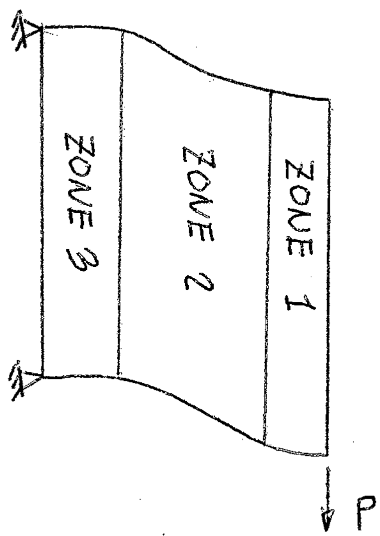

Figure 18. Four Corner Fixed Diaphragm

REFERENCES

(1) "Strength and Stiffness of Steel Deck Subjected to In-Plane Loading." Civil Engineering Studies, Report No. 2011. West Virginia University, 1970.

(2) Beaufait, Fred W. Computer Methods of Structural Analysis. New York: McGraw-Hill Book Company, 1970, pp. 447-477.

(3) Bryan, E. R. and W. M. El-Dakhakhni. "Shear Flexibility and Strength of Corrugated Decks." Journal of the Structural Division, ASCE, Vol. 119, No. ST 11 (November, 1968), pp. 2549-2580.

(4) Easley, J. T. and D. E. McFarland. "Buckling of Light Gage Corrugated Metal Shear Diaphragms." Journal of the Structural Division, ASCE, Vol. 128, No. ST 7 (July, 1969), p. 1497.

(5) Pekoz, T. B. and G. Winter. "Torsional-Flexural Buckling of Thin-Walled Sections Under Eccentric Load." Journal of the Structural Division, ASCE, Vol. 95, No. ST 5 (May, 1969), p. 1349.

(6) Bryan, E. R. and W. M. Dakhakhni. "Shear of Thin Plates With Flexible Edge Members." Journal of the Structural Division, ASCE, Vol. 90, No. ST 4 (August, 1964), pp. 1-14.

APPENDIX

"STRUDL" COMPUTER INPUT LIST

Truss Configurations

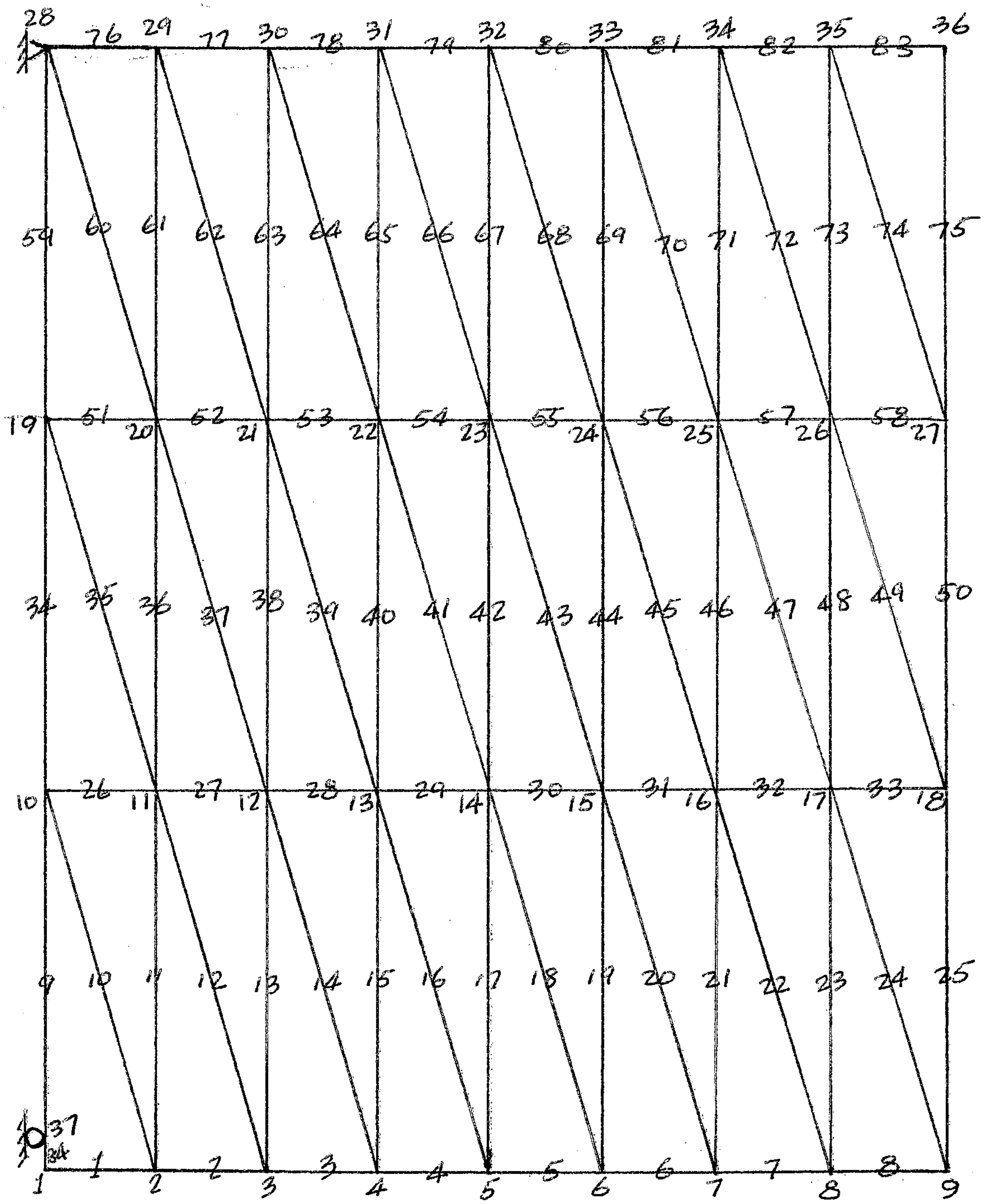

Figure 19. Typical Configuration of Truss Analogy

Joint Coordinates

Joint No.	X	Y	Joint No.	X	Y
1	0.0	0.0	33	120.0	240.0
2	24.0	0.0	34	144.0	240.0
3	48.0	0.0	35	168.0	240.0
4	72.0	0.0	36	192.0	240.0
5	96.0	0.0	37	0.0	4.0
6	120.0	0.0			
7	144.0	0.0			
8	168.0	0.0			
9	192.0	0.0			
10	0.0	80.0			
11	24.0	80.0			
12	48.0	80.0			
13	72.0	80.0			
14	96.0	80.0			
15	120.0	80.0			
16	144.0	80.0			
17	168.0	80.0			
18	192.0	80.0			
19	0.0	160.0			
20	24.0	160.0			
21	48.0	160.0			
22	72.0	160.0			
23	96.0	96.0			
24	120.0	120.0			
25	144.0	144.0			
26	168.0	168.0			
27	192.0	192.0			
28	0.0	0.0			
29	24.0	24.0			
30	48.0	48.0			
31	72.0	72.0			
32	96.0	96.0			

```
CARD
  1   TYPE PLANE FRAME
  2   UNITS KIP IN
  3   CONSTANTS E 29000 ALL
  4   JOINT COORD
  5   1 0 0
  6   2 24 0
  7   3 48 0
  8   4 72 0
  9   5 96 0
 10   6 120 0
 11   7 144 0
 12   8 168 0
 13   9 192 0
 14   10 0 80
 15   11 24 80
 16   12 48 80
 17   13 72 80
 18   14 96 80
 19   15 120 80
 20   16 144 80
 21   17 168 80
 22   18 192 80
 23   19 0 160
 24   20 24 160
 25   21 48 160
 26   22 72 160
 27   23 96 160
 28   24 120 160
 29   25 144 160
 30   26 168 160
 31   27 192 160
 32   28 0 240 S
 33   29 24 240
 34   30 48 240
 35   31 72 240
 36   32 96 240
 37   33 120 240
 38   34 144 240
 39   35 168 240
 40   36 192 240
 41   37 0 4 S
 42   JOINT REL
 43   28 MOM Z
 44   37 FOR Y MOM Z
 45   MEM INC
 46   1 1 2
 47   2 2 3
 48   3 3 4
 49   4 4 5
 50   5 5 6
 51   6 6 7
 52   7 7 8
 53   8 8 9
 54   9 37 10
```

CARD			
55	10	2	10
56	11	2	11
57	12	3	11
58	13	3	12
59	14	4	12
60	15	4	13
61	16	5	13
62	17	5	14
63	18	6	14
64	19	6	15
65	20	7	15
66	21	7	16
67	22	8	16
68	23	8	17
69	24	9	17
70	25	9	18
71	26	10	11
72	27	11	12
73	28	12	13
74	29	13	14
75	30	14	15
76	31	15	16
77	32	16	17
78	33	17	18
79	34	10	19
80	35	11	19
81	36	11	20
82	37	12	20
83	38	12	21
84	39	13	21
85	40	13	22
86	41	14	22
87	42	14	23
88	43	15	23
89	44	15	24
90	45	16	24
91	46	16	25
92	47	17	25
93	48	17	26
94	49	18	26
95	50	18	27
96	51	19	20
97	52	20	21
98	53	21	22
99	54	22	23
100	55	23	24
101	56	24	25
102	57	25	26
103	58	26	27
104	59	19	28
105	60	20	28
106	61	20	29
107	62	21	29
108	63	21	30

```
CARD
 109   64 22 30
 110   65 22 31
 111   66 23 31
 112   67 23 32
 113   68 24 32
 114   69 24 33
 115   70 25 33
 116   71 25 34
 117   72 26 34
 118   73 26 35
 119   74 27 35
 120   75 27 36
 121   76 28 29
 122   77 29 30
 123   78 30 31
 124   79 31 32
 125   80 32 33
 126   81 33 34
 127   82 34 35
 128   83 35 36
 129   84 1 37
 130   MEM PROP PRISM AX 6.2 IZ 10.8
 131   1
 132   2
 133   3
 134   4
 135   5
 136   6
 137   7
 138   8
 139   9
 140   34
 141   59
 142   84
 143   75
 144   50
 145   25
 146   76
 147   77
 148   78
 149   79
 150   80
 151   81
 152   82
 153   83
 154   MEM PROP PRISM AX 3.09 IZ 0.865
 155   26
 156   27
 157   28
 158   29
 159   30
 160   31
 161   32
 162   33
```

```
CARD
 163  51
 164  52
 165  53
 166  54
 167  55
 168  56
 169  57
 170  58
 171  MEM PROP PRISM AX 0.168 IZ 0.1
 172  10
 173  11
 174  12
 175  13
 176  14
 177  15
 178  16
 179  17
 180  18
 181  19
 182  20
 183  21
 184  22
 185  23
 186  24
 187  35
 188  36
 189  37
 190  38
 191  39
 192  40
 193  41
 194  42
 195  43
 196  44
 197  45
 198  46
 199  47
 200  48
 201  49
 202  60
 203  61
 204  62
 205  63
 206  64
 207  65
 208  66
 209  67
 210  68
 211  69
 212  70
 213  71
 214  72
 215  73
 216  74
```

```
CARD
 217   MEM REL
 218   10 STA MOM Z END MOM Z
 219   11 STA MOM Z END MOM Z
 220   12 STA MOM Z END MOM Z
 221   13 STA MOM Z END MOM Z
 222   14 STA MOM Z END MOM Z
 223   15 STA MOM Z END MOM Z
 224   16 STA MOM Z END MOM Z
 225   17 STA MOM Z END MOM Z
 226   18 STA MOM Z END MOM Z
 227   19 STA MOM Z END MOM Z
 228   20 STA MOM Z END MOM Z
 229   21 STA MOM Z END MOM Z
 230   22 STA MOM Z END MOM Z
 231   23 STA MOM Z END MOM Z
 232   24 STA MOM Z END MOM Z
 233   25 STA MOM Z
 234   26 STA MOM Z
 235   33 END MOM Z
 236   35 STA MOM Z END MOM Z
 237   36 STA MOM Z END MOM Z
 238   37 STA MOM Z END MOM Z
 239   38 STA MOM Z END MOM Z
 240   39 STA MOM Z END MOM Z
 241   40 STA MOM Z END MOM Z
 242   41 STA MOM Z END MOM Z
 243   42 STA MOM Z END MOM Z
 244   43 STA MOM Z END MOM Z
 245   44 STA MOM Z END MOM Z
 246   45 STA MOM Z END MOM Z
 247   46 STA MOM Z END MOM Z
 248   47 STA MOM Z END MOM Z
 249   48 STA MOM Z END MOM Z
 250   49 STA MOM Z END MOM Z
 251   51 STA MOM Z
 252   58 END MOM Z
 253   60 STA MOM Z END MOM Z
 254   61 STA MOM Z END MOM Z
 255   62 STA MOM Z END MOM Z
 256   63 STA MOM Z END MOM Z
 257   64 STA MOM Z END MOM Z
 258   65 STA MOM Z END MOM Z
 259   66 STA MOM Z END MOM Z
 260   67 STA MOM Z END MOM Z
 261   68 STA MOM Z END MOM Z
 262   69 STA MOM Z END MOM Z
 263   70 STA MOM Z END MOM Z
 264   71 STA MOM Z END MOM Z
 265   72 STA MOM Z END MOM Z
 266   73 STA MOM Z END MOM Z
 267   74 STA MOM Z END MOM Z
 268   76 STA MOM Z
 269   83 END MOM Z
 270   84 STA MOM Z
```

```
LOADING '1' '4.55'
JOINT LOAD
9 FOR Y -6.0
INACT MEM 42 19 21 40 44 63 65
STIFFN ANALYSIS
LIST FOR DISP ALL
FINISH
```

VITA

Shen-Sheng A. Chou

Candidate for the Degree of

Master of Science

Report: TRUSS-ANALOGY METHOD FOR THE ANALYSIS OF STEEL DIAPHRAGM

Major Field: Civil Engineering

Biographical:

Personal Data: Born September 25, 1948, in Sheng-hai, China, the son of Mr. and Mrs. C. H. Chou.

Education: Received the Diploma from Taiwan Provincial Taipei Institute of Technology, Taipei, Taiwan, in June, 1969; completed the requirements for the Master of Science degree in December, 1974.